

# Double deeply virtual Compton scattering off the nucleon

M. Guidal<sup>1</sup> and M. Vanderhaeghen<sup>2</sup>

<sup>1</sup>*Institut de Physique Nucléaire, F-91406 Orsay, France*

<sup>2</sup>*Institut für Kernphysik, Johannes Gutenberg Universität, D-55099 Mainz, Germany*

We study the double deeply virtual Compton scattering (DDVCS) process off the nucleon, through the scattering of a spacelike virtual photon with large virtuality resulting in the production of a timelike virtual photon, decaying into an  $e^+e^-$  pair. This process is expressed in the Bjorken regime in terms of generalized parton distributions (GPDs) and it is shown that by varying the invariant mass of the lepton pair, one can directly extract the GPDs from the observables. We give predictions for the DDVCS cross section and beam helicity asymmetry and discuss its experimental feasibility.

PACS numbers: 13.60.Fz, 12.38.Bx, 13.60.Le

The understanding of hadron structure in terms of quark and gluon degrees of freedom, remains an outstanding challenge. An important source of information is provided by experiments involving electroweak probes. In this way, elastic form factors as well as quark and gluon distributions in the nucleon have been mapped out in quite some detail. In recent years, a whole new class of hard exclusive reactions have become accessible both theoretically and experimentally to study hadron structure. In particular, the deeply virtual Compton scattering (DVCS) and hard electroproduction of meson processes are at present under investigation at different facilities (HERMES [1], JLab [2], HERA [3, 4]), or will be addressed by experiments in the near future. In these processes, a highly virtual photon (with large virtuality  $Q^2$ ) scatters from the nucleon and a real photon (in the case of DVCS) or a meson is produced. Due to the large scale  $Q^2$  involved, these hard exclusive processes are factorizable in a hard part, which can be calculated from perturbative QCD, and a soft part, which contains the information on nucleon structure and is parametrized in terms of generalized parton distributions (GPDs) (see Refs. [5, 6, 7] for reviews and references therein).

The GPDs depend upon the different longitudinal momentum fractions  $x+\xi$  ( $x-\xi$ ) of the initial (final) quarks (see upper left panel of Fig. 1). As the momentum fractions of the initial and final quarks are different, in contrast to the forward parton distributions, one accesses in this way quark momentum correlations in the nucleon, which are at present largely unknown. Furthermore, sum rule integrals of GPDs over  $x$  provide new nucleon structure information and are also amenable to lattice QCD calculations for direct comparison. In particular, the second moment of a particular combination of GPDs gives access to the total angular momentum carried by quarks in the nucleon [8]. Such a quantity would be highly complementary to the information extracted from polarized deep-inelastic scattering experiments, which found that about 20 - 30 % of the nucleon spin originates from the quark intrinsic spins (see Ref. [9] for a recent review).

To obtain these new informations, one of the main challenges is to directly extract the GPDs from observables.

In the DVCS or hard exclusive meson electroproduction observables, the GPDs enter in general in convolution integrals over the average quark momentum fraction  $x$ , so that only  $\xi$  (half the difference of both quark momentum fractions) can be accessed experimentally. A particular exception is when one measures an observable proportional to the imaginary part of the amplitude, such as the beam helicity asymmetry in DVCS. Then, one actually measures directly the GPDs at some specific point,  $x = \xi$ , which is certainly an important gain of information but clearly not sufficient to map out the GPDs independently in both quark momentum fractions, which is needed to construct sum rules. In absence of any model-independent “deconvolution” procedure at this moment, existing analyses of DVCS experiments have to rely on some global model fitting procedure.

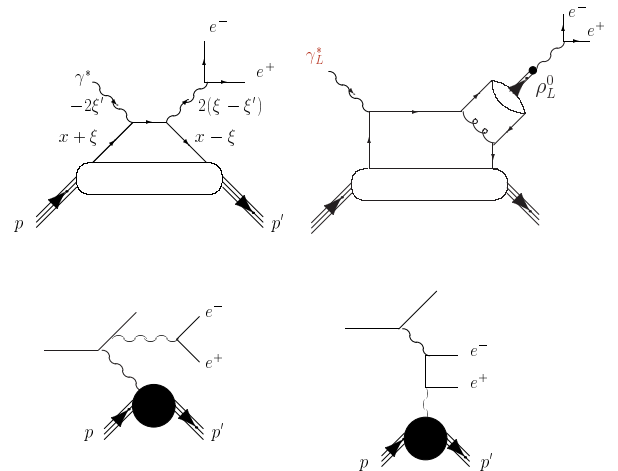


FIG. 1: Diagrams for the  $lp \rightarrow lpe^+e^-$  process : DDVCS process (upper left), vector meson (VM) production process (upper right), Bethe-Heitler (BH) processes (lower two diagrams). Crossed diagrams are not shown but also included.

The double DVCS (DDVCS) process, i.e. the scattering of a spacelike virtual photon from the nucleon with the production of a virtual photon in the final state, provides a way around this problem of principle. Compared to the DVCS process with a real photon in the final state, the virtuality of the final photon in DDVCS yields an

additional lever arm, which allows to vary both quark momenta  $x$  and  $\xi$  independently. This additional lever arm of the DDVCS compared to the DVCS process has already been noted in Refs. [10, 11, 12]. Also, the lepton pair production process induced by a real photon, i.e. the  $\gamma p \rightarrow e^+e^-p$  reaction has been studied [13]. In this letter, we provide the first numerical estimates of the DDVCS and its competing processes and show how the GPDs can be directly extracted from DDVCS observables.

The DDVCS process can be accessed through the  $lp \rightarrow lpe^+e^-$  reaction, which is characterized by the four-momenta :  $k$  ( $k'$ ) of the incoming (scattered) leptons  $l$ ,  $p$  ( $p'$ ) of the initial (final) nucleons, and  $l_e^-, l_e^+$  of the leptons in the produced  $e^+e^-$  pair.

To see how the DDVCS process can yield more complete information of GPDs than the DVCS process, one first has to discuss its richer kinematics. The DDVCS process is characterized by 8 independent kinematical variables. Firstly, there are the same 5 kinematical variables which specify the DVCS process and which we choose as : the initial beam energy  $E_e$ ; the virtuality  $Q^2$  of the incoming photon in the upper left diagram of Fig. 1, i.e.  $Q^2 \equiv -q^2$ , where  $q \equiv k - k'$ ; the usual Bjorken variable  $x_B \equiv Q^2/(2p \cdot q)$ ; the four-momentum transfer to the nucleon  $t \equiv \Delta^2$ , where  $\Delta \equiv p' - p$ ; and the out-of-plane angle  $\Phi$  between the production plane, spanned by the vectors  $\vec{q}$  and  $\vec{q}'$ , and the scattering plane spanned by the vectors  $\vec{k}$  and  $\vec{k}'$ . Furthermore, one needs 3 additional variables to fully characterize the DDVCS process which we choose as : the virtuality  $q'^2 \equiv (l_{e^-} + l_{e^+})^2$  of the produced  $e^+e^-$  pair; and the 2 angles of one lepton of the produced lepton pair, evaluated in the  $c.m.$  system of the  $e^+e^-$  pair, and which span the solid angle  $d\Omega_{e^+e^-}^*$ .

At large  $Q^2$ , we calculate the DDVCS process in the handbag approximation as shown in Fig. 1 (upper left diagram), which yields the amplitude :

$$\begin{aligned}
H_{\text{DDVCS}}^{\mu\nu} &= \frac{1}{2} (-g^{\mu\nu})_{\perp} \\
&\times \int_{-1}^{+1} dx C^+(x, \xi, \xi') \left[ H^P(x, \xi, t) \bar{N}(p') \not{n} N(p) \right. \\
&\quad \left. + E^P(x, \xi, t) \bar{N}(p') i\sigma^{\kappa\lambda} \frac{n_{\kappa} \Delta_{\lambda}}{2m_N} N(p) \right] \\
&+ \frac{i}{2} (\epsilon^{\nu\mu})_{\perp} \\
&\times \int_{-1}^{+1} dx C^-(x, \xi, \xi') \left[ \tilde{H}^P(x, \xi, t) \bar{N}(p') \not{n} \gamma_5 N(p) \right. \\
&\quad \left. + \tilde{E}^P(x, \xi, t) \bar{N}(p') \gamma_5 \frac{\Delta \cdot n}{2m_N} N(p) \right], \quad (1)
\end{aligned}$$

where  $\mu$  ( $\nu$ ) refer to the four-vector indices of the incoming spacelike (outgoing timelike) virtual photons respectively,  $n$  is a light-like vector along the direction of the incoming virtual photon, and where we refer to Ref. [7] for the expressions of the symmetrical (antisymmetrical) twist-2 tensors  $g_{\perp}^{\mu\nu}$  ( $\epsilon_{\perp}^{\mu\nu}$ ). Furthermore, in Eq. (1),

$N(p), N(p')$  represent the nucleon spinors and  $m_N$  is the nucleon mass. The GPDs  $H, E, \tilde{H}, \tilde{E}$  in Eq. (1) are the same as in the DVCS case, and depend on the arguments  $x, \xi$ , and  $t$ , with  $x$  and  $\xi$  as defined in Fig. 1. The coefficient functions  $C^{\pm}$  in the DDVCS amplitude of Eq. (1) take the form :

$$C^{\pm}(x, \xi, \xi') = \frac{1}{x - (2\xi' - \xi) + i\varepsilon} \pm \frac{1}{x + (2\xi' - \xi) - i\varepsilon}, \quad (2)$$

where  $-2\xi'$  and  $2(\xi - \xi')$  are the longitudinal momentum fractions of the incoming spacelike and outgoing timelike virtual photons respectively (see Fig. 1). In the large  $Q^2$  limit, one has  $2\xi' \rightarrow x_B/(1 - x_B/2)$ . The difference  $(2\xi' - \xi)$  appearing in the quark propagators in Eq. (2) can be expressed as (relative to  $\xi$ ) :

$$\begin{aligned}
\frac{2\xi' - \xi}{\xi} &= \frac{1 - (q'^2 - \Delta^2)/Q^2 + 8\xi'^2 \bar{m}^2/Q^2}{1 + (q'^2 - \Delta^2)/Q^2} \\
&\rightarrow \frac{1 - q'^2/Q^2}{1 + q'^2/Q^2}, \quad (3)
\end{aligned}$$

with  $\bar{m}^2 = m_N^2 - \Delta^2/4$ . For the DDVCS process, by varying the virtualities of both incoming and outgoing virtual photons, one can vary independently the variables,  $\xi$  and  $\xi'$ , whereas, in DVCS, only one variable can be varied as  $\xi \approx \xi'$ . One then sees from Eqs. (1,2) that the imaginary part of the DDVCS amplitude (which can be directly measured through the beam helicity asymmetry as discussed further on) will access, in a concise notation, the GPD  $(2\xi' - \xi, \xi, t)$ , and allows to map out the GPDs as function of its three arguments independently. In the second line in Eq. (3), we have indicated the expression in the large  $Q^2$  limit, which is displayed in Fig. 2. For

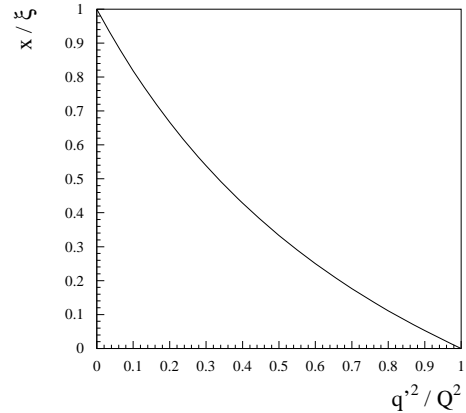


FIG. 2: Range in the argument  $x = 2\xi' - \xi$  (relative to  $\xi$ ) of the GPD  $(x, \xi, t)$  which one accesses by measuring the imaginary part of the DDVCS process at different values of the lepton invariant mass  $q'^2$  (relative to the initial virtuality  $Q^2$ ).

a timelike virtual photon (i.e.  $q'^2 > 0$ ), one can only access the  $x < \xi$  region in the arguments  $(x, \xi, t)$  of the GPDs because, for kinematical reasons,  $q'^2/Q^2$  will always be less than 1. Therefore, the imaginary part of

the DDVCS amplitude maps out the GPD where its first argument lies in the range  $0 < 2\xi' - \xi < \xi$ . In particular, when  $q'^2$  is varied from 0 to  $Q^2/2$ , the argument  $x$  spans about 2/3 of the range  $[x, \xi]$ . Although one does not access the whole range in  $x$ , clearly, the gain of information on the GPDs is tremendous as no deconvolution is involved to access this region of the GPDs. Furthermore,  $x < \xi$  is just the range where the GPDs contain wholly new information on mesonic ( $q\bar{q}$ ) components of the nucleon, which is absent in the forward limit (where  $\xi = 0$ ). To access the range  $x > \xi$  one would need two spacelike virtual photons, necessitating to select the two-photon exchange process in elastic electron nucleon scattering.

Besides the DDVCS process, the  $lp \rightarrow lpe^+e^-$  reaction contains two classes of Bethe-Heitler (BH) processes as shown in Fig. 1. The BH processes are fully calculable as they involve elastic nucleon form factors. Furthermore, the outgoing timelike photon which couples pointlike to the quark line in the DDVCS process can also originate from a neutral vector meson (VM) which couples to the quark line through a one-gluon exchange (upper right diagram in Fig. 1). For the contamination of the VM production, we estimate it by the leading order amplitude for the hard electroproduction of longitudinally polarized VM [14]. For this process, which is of order  $\mathcal{O}(\alpha_s)$  in the strong coupling constant compared to the handbag process, a factorization theorem has been proved [15], allowing to express its amplitude also in terms of GPDs.

In the following, we will estimate the coherent sum of all these processes. The fully differential cross section of the  $lp \rightarrow lpe^+e^-$  reaction can then be expressed as :

$$\frac{d\sigma}{dQ^2 dx_B dt d\Phi dq'^2 d\Omega_{e^-}^*} = \frac{1}{(2\pi)^4} \cdot \frac{x_B y^2}{32 Q^4 \left(1 + \frac{4m_N^2 x_B^2}{Q^2}\right)^{1/2}} \times \frac{1}{(4\pi)^3} \left| T_{BH} + T_{DDVCS} + T_{VM} \right|^2, \quad (4)$$

where  $y \equiv (p.q)/(p.k)$ , and where  $T_{BH}$ ,  $T_{DDVCS}$ , and  $T_{VM}$  are the amplitudes for the BH, DDVCS and VM processes respectively. When integrating Eq. (4) over the angles of the produced  $e^+e^-$  pair, the resulting DDVCS cross section reduces in the limit  $q'^2 \rightarrow 0$  to :

$$\frac{d\sigma}{dQ^2 dx_B dt d\Phi dq'^2} \rightarrow \left( \frac{d\sigma}{dQ^2 dx_B dt d\Phi} \right) \cdot \frac{N}{q'^2}, \quad (5)$$

where the DVCS cross section appears on the *rhs* of Eq. (5). The factor  $N$  in Eq. (5) is given by

$$N = \frac{\alpha_{em}}{4\pi} \cdot \frac{4}{3}, \quad (6)$$

where  $\alpha_e \approx 1/137$  is the fine structure constant, introduced by the decay of the outgoing photon into the lepton pair. One sees that the downside of the DDVCS process is that it involves small cross sections : at a virtuality

$q'^2 = 1 \text{ GeV}^2$ , the DDVCS cross section is reduced by at least a factor  $N^{-1}$  ( $\approx 1.3 \times 10^3$ ) compared to the DVCS cross section. At lower values of  $q'^2$ , the DDVCS cross section rises however as  $1/q'^2$ .

Besides the DDVCS cross section, a particularly informative observable is obtained by scattering a longitudinally polarized lepton beam and flipping its helicity. The resulting single spin asymmetry (SSA) originates from the interference of the DDVCS and BH processes as :

$$SSA \sim \text{Im} \left[ T_{BH} (T_{DDVCS} + T_{VM})^* \right]. \quad (7)$$

Because the BH process is real, the SSA accesses the imaginary part of the DDVCS + VM process, which is proportional to the GPD( $2\xi' - \xi, \xi, t$ ) (see Eqs. (1,2)).

In Fig. 3, we show the  $q'^2$  dependence of the estimated

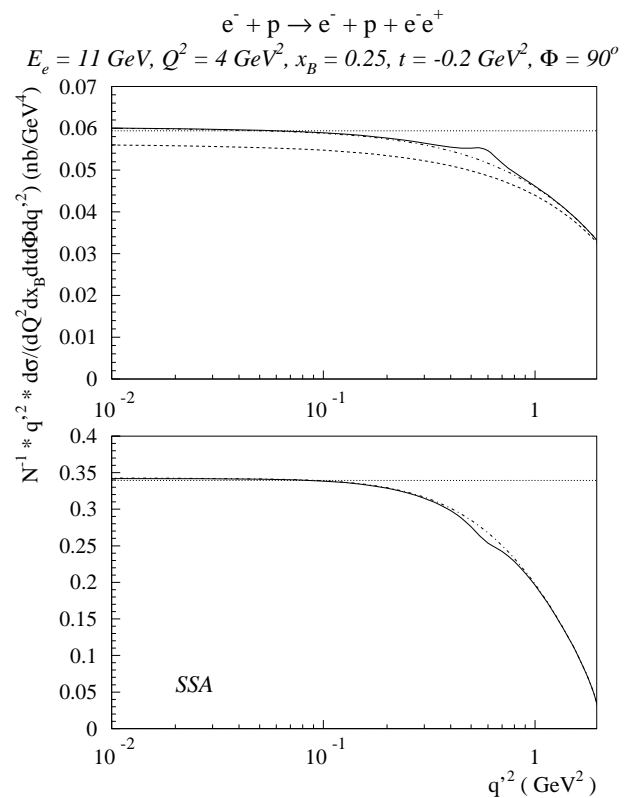


FIG. 3: Cross section (upper panel) and SSA (lower panel) of the  $ep \rightarrow epe^+e^-$  process as function of the  $e^+e^-$  virtuality  $q'^2$ . Dashed curves : BH processes; dashed-dotted curves : BH + DDVCS processes, full curves : BH + DDVCS +  $\rho_L^0$  processes. The dotted curves are the corresponding results for the  $ep \rightarrow epr\gamma$  proces. The  $ep \rightarrow epe^+e^-$  cross section is scaled with  $N^{-1} \cdot q'^2$ , in order to reproduce exactly the  $ep \rightarrow epr\gamma$  cross section in the limit  $q'^2 \rightarrow 0$ , according to Eq. (5).

cross section and SSA for the  $ep \rightarrow epe^+e^-$  process in kinematics accessible at JLab. As the twist-2 SSA basically displays a  $\sin \Phi$  structure, we show its value at  $\Phi = 90^\circ$ . For the GPDs, we use a  $\xi$ -dependent parametrization (see Refs. [7, 14]), using the MRST01 [16] forward quark distributions as input. As is seen from Fig. 3,

we firstly confirm numerically that the  $ep \rightarrow epe^+e^-$  cross section scaled with the factor  $N^{-1}q'^2$  reduces to the  $ep \rightarrow ep\gamma$  cross section when approaching the real photon point. Similarly, the SSA for the  $ep \rightarrow epe^+e^-$  process reduces to the corresponding SSA for the  $ep \rightarrow ep\gamma$  process. When going to larger virtualities  $q'^2$ , the DDVCS shows a growing deviation from the  $1/q'^2$  behavior and the magnitude of the SSA decreases. Furthermore, we show in Fig. 3 the contribution of the  $\rho_L^0 \rightarrow e^+e^-$  process (upper right diagram of Fig. 1), which is the most pronounced VM process. We find that, except in the immediate vicinity of  $q'^2 \approx m_\rho^2$ , the  $\rho_L^0 \rightarrow e^+e^-$  process is very small. This can be understood because the cross section for the  $\rho_L^0 \rightarrow e^+e^-$  process is reduced by a factor  $\alpha_{em}^2$  compared to the  $\rho_L^0$  process, whereas the DDVCS cross section is only reduced by a factor  $\alpha_{em}$  compared to the DVCS cross section. Similarly, the SSA is only slightly affected by the VM process and is dominantly proportional to the imaginary part of the DDVCS process according to Eq. (7). The strong sensitivity of the SSA on  $q'^2$ , as seen from Fig. 3, should therefore allow to map out the GPDs in the range  $x < \xi$ .

Fig. 4 shows the comparison between the  $ep \rightarrow ep(\gamma, \rho_L^0)$  and  $ep \rightarrow ep(\gamma, \rho_L^0) \rightarrow ep(e^+e^-)$  processes for a typical kinematics accessible at JLab at 6 GeV. Whereas the  $ep \rightarrow ep\rho_L^0$  process is roughly comparable to the DVCS + BH one for these kinematics, their “timelike” analogues, show that the  $\rho_L^0$  channel is suppressed by 2 orders of magnitude with respect to the DDVCS+BH.

Given that about  $10^4$  DVCS+BH events were measured recently at CLAS [2] in an effective 4-day data taking period at a luminosity of  $10^{34}cm^{-2}s^{-1}$  in a non-dedicated experiment, it can certainly be envisaged that the DDVCS+BH cross section, which is about 3 orders of magnitude lower, be measured with a dedicated long-time experiment. A luminosity of  $10^{35}cm^{-2}s^{-1}$ , projected at CLAS for the upgrade of JLab at 12 GeV, or at a future dedicated lepton facility, would allow to measure this reaction with reasonable statistics.

In conclusion, we have studied the DDVCS process with the production of a timelike virtual photon, decaying into an  $e^+e^-$  pair. We have expressed the DDVCS amplitude in terms of GPDs and have shown that by varying the virtuality  $q'^2$  of the timelike photon, one can map out the GPDs as function of both initial and final quark momentum fractions. We have given cross section estimates for the DDVCS and its associated processes. Although the cross sections are small, their measurement seems feasible with a dedicated experiment at JLab and at a future high-energy, high-luminosity lepton facility. Of particular interest is the SSA using a polarized lepton beam. We have shown that by measuring the SSA, one can directly extract the GPDs in the domain where one is sensitive to  $q\bar{q}$  correlations in the nucleon, providing a whole new source of nucleon structure information which is absent in forward quark distributions.

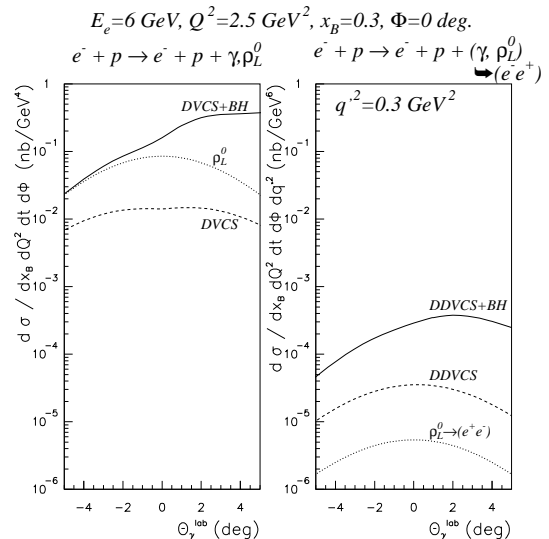


FIG. 4: Comparison of the different cross sections (as indicated on the curves) for the  $ep \rightarrow ep(\gamma, \rho_L^0)$  (left panel) and  $ep \rightarrow ep e^+e^-$  (right panel) reactions in JLab kinematics.

This work was supported by the Deutsche Forschungsgemeinschaft (SFB443), by the CNRS/IN2P3, and in part by the European Commission IHP program (contract HPRN-CT-2000-00130).

- 
- [1] A. Airapetian *et al.* (HERMES Collaboration), Phys. Rev. Lett. **87**, 182001 (2001).
  - [2] S. Stepanyan *et al.* (CLAS Collaboration), Phys. Rev. Lett. **87**, 182002 (2001).
  - [3] C. Adloff *et al.* (H1 Collaboration), Phys. Lett. B **517**, 47 (2001).
  - [4] F.R. Saull (ZEUS Collaboration), Proc. ICHEP 1999, (Tampere, Finland, July 1999), hep-ex/0003030.
  - [5] X. Ji, J. Phys. G **24**, 1181 (1998).
  - [6] A.V. Radyushkin, in the Boris Ioffe Festschrift 'At the Frontier of Particle Physics / Handbook of QCD', edited by M. Shifman (World Scientific, Singapore, 2001).
  - [7] K. Goeke, M.V. Polyakov, M. Vanderhaeghen, Prog. Part. Nucl. Phys. **47**, 401 (2001).
  - [8] X. Ji, Phys. Rev. Lett. **78**, 610 (1997).
  - [9] B.W. Filippone and X. Ji, Adv.Nucl.Phys. **26**, 1 (2001).
  - [10] D. Müller, D. Robaschik, B. Geyer, F.-M. Dittes, and J. Horejsi, Fortschr. Phys. **42**, 101 (1994).
  - [11] J. Blumlein, D. Robaschik, Nucl.Phys. **B 581** 449 (2000).
  - [12] A.V. Belitsky, D. Müller, and A. Kirchner, Nucl. Phys. **B629**, 323 (2002).
  - [13] E.R. Berger, M. Diehl, B. Pire, Eur. Phys. J. C **23**, 675 (2002).
  - [14] M. Vanderhaeghen, P.A.M. Guichon, and M. Guidal, Phys. Rev. Lett. **80**, 5064 (1998); Phys. Rev. D **60**, 094017 (1999).
  - [15] J.C. Collins, L.L. Frankfurt, and M. Strikman, Phys. Rev. D **56**, 2982 (1997).
  - [16] A.D. Martin, R.G. Roberts, W.J. Stirling, R.S. Thorne, Eur. Phys. J. C **23**, 73 (2002).